Published in final edited form as:
Biomaterials. 2010 August ; 31(22): 5903–5910. doi:10.1016/j.biomaterials.2010.03.062.

Chitosan-alginate 3D scaffolds as a mimic of the glioma tumor microenvironment

Forrest M. Kievit[a], **Stephen J. Florczyk**[a], **Matthew Leung**[a], **Omid Veiseh**[a], **James O. Park**[b], **Mary L. Disis**[c], and **Miqin Zhang**[a,*]

[a]Department of Materials Science & Engineering, University of Washington, Seattle, WA 98195, USA

[b]Department of Surgery, University of Washington, Seattle, WA 98195, USA

[c]Division of Oncology, University of Washington, Seattle, WA 98195. USA

Abstract

Despite recent advances in the understanding of its cell biology, glioma remains highly lethal. Development of effective therapies requires a cost-effective *in vitro* tumor model that more accurately resembles the *in vivo* tumor microenvironment as standard two-dimensional tissue culture conditions do so poorly. Here we report on the use of a three-dimensional (3D) chitosanalginate (CA) scaffold to serve as an extracellular matrix that promotes the conversion of cultured cancer cells to a more malignant *in vivo*-like phenotype. Human U-87 MG and U-118 MG glioma cells and rat C6 glioma cells were chosen for study. *In vitro* tumor cell proliferation and secretion of factors that promote tumor malignancy, including VEGF, MMP-2, fibronectin, and laminin, were assessed. The scaffolds pre-cultured with U-87 MG and C6 cells were then implanted into nude mice to evaluate tumor growth and blood vessel recruitment compared to the standard 2D cell culture and 3D Matrigel matrix xenograft controls. Our results indicate that while the behavior of C6 cells showed minimal differences due to their highly malignant and invasive nature, U-87 MG and U-118 MG cells exhibited notably higher malignancy when cultured in CA scaffolds. CA scaffolds provide a 3D microenvironment for glioma cells that is more representative of the *in vivo* tumor, thus can serve as a more effective platform for development and study of anticancer therapeutics. This unique CA scaffold platform may offer a valuable alternative strategy to the time-consuming and costly animal studies for a wide variety of experimental designs.

Keywords

chitosan; alginate; natural polymer; scaffold; tumor microenvironment; glioma

1. Introduction

Gliomas are the most common and lethal type of brain cancer, accounting for 80% of brain tumors, with a 2-year survival of 17–43% [1]. Recent advances in the understanding of glioma

*Corresponding author: Miqin Zhang, Department of Materials Science and Engineering, University of Washington, 302L Roberts Hall, Box 352120, Seattle, WA 98195, USA. Telephone: 206-616-9356; Fax: 206-543-3100; mzhang@u.washington.edu.

biology have revealed effective therapeutic targets, translating to improved patient outcomes [2]. Despite these improvements, the development of anticancer drugs has been hindered by the lack of effective tumor models that closely mimic the human disease [3].

Standard two-dimensional cell line cultures provide researchers a convenient *in vitro* platform for drug development. However, cells cultured on flat Petri dish surfaces do not ideally represent *in vivo* conditions, as these cells display a dramatically reduced malignant phenotype when compared to the tumor *in vivo* [4,5]. Hence, *in vitro* results often do not translate well to *in vivo* systems. There is a pressing need for better *in vitro* models of human cancer that will allow researchers to reduce *in vivo* experiments by *in vitro* pre-testing that will defray costs, shorten experimental time, provide a much more controllable environment, and reduce loss of animal life.

Three-dimensional (3D) culture systems are designed to bridge the gap between *in vitro* and *in vivo* cancer models [8–11]. These 3D systems are intended to increase cancer cell malignancy and retain the *in vivo* phenotype, by mimicking the structure of the tumor microenvironment [12]. Natural extracellular matrix materials such as collagen, fibrin, and the commercially available Matrigel matrix (BD Biosciences) have been used, but these animal-source products are expensive, and can potentially transmit pathogens [10]. Synthetic polymers such as poly (lactide-co-glycolide) (PLGA) have also been studied [9,13], but they can release acidic degradation products that are toxic to cells, and negatively affect experimental results. Chitosan and alginate, two non-mammalian sourced, natural polymers, are ideally suited as scaffold materials due to their biocompatibility and lack of immunogenicity [14,15]. Chitosanalginate complex (CA) scaffolds have previously been shown to provide an ideal growth environment for cartilage and bone regeneration [16,17], and stem cell renewal [18]. In this study, we show that CA scaffolds can be used to better mimic the tumor microenvironment of glioma *in vitro* by promoting a more malignant phenotype. These tumors were developed *in vitro* by seeding U-87 MG and U-118 MG human glioma cells on CA scaffolds. As a comparison we also tested a cancer stem-like cell line (C6 rat glioma), which is known to be highly invasive and tumorigenic [19–22]. Developed tumor malignancy was assessed by ELISA and dot blot analyses of secreted key growth factors and extracellular matrix. Further assessment of *in vitro* developed U-87 MG tumors was performed by implantation into mice and monitoring tumor growth and blood vessel formation. *In vitro* tumors from C6 cells were also implanted as a control.

2. Materials and Methods

2.1 Materials

All chemicals were purchased from Sigma-Aldrich (St. Louis, MO) unless otherwise specified. Chitosan (PolySciences, PA, 15,000 MW) and sodium alginate powders were used as received. Dulbecco's Modified Eagle Medium (DMEM), Antibiotic-antimycotic, Dulbecco's phosphate buffered saline (D-PBS), and Alamar Blue reagent were purchased from Invitrogen (Carlsbad, CA). Fetal bovine serum (FBS) was purchased from Atlanta Biologicals (Atlanta, GA). C6 rat glioma, U-87 MG human glioma, and U-118 MG human glioma cell lines and Minimum Essential Media (MEM) were purchased from American Type Culture Collection (ATCC, Manassas, VA). Cells were maintained according to manufacturer's instructions in fully supplemented DMEM (C6 and U-118 MG) or MEM (U-87 MG) with 10% FBS and 1% antibiotic-antimycotic) at 37°C and 5% CO_2 in a fully humidified incubator. Reduced growth factor matrigel matrix was purchased from BD Biosciences (San Jose, CA). VEGF and MMP-2 ELISA kits were purchased from R&D Systems (Minneapolis, MN).

2.2 CA scaffold synthesis

CA scaffolds were prepared as previously reported [16,17]. Briefly, a 4 wt% chitosan and 2 wt% acetic acid solution was mixed under constant stirring in a blender for 7 minutes to obtain a homogeneous chitosan solution. A 4 wt% alginate solution was added to the chitosan solution, and mixed in a blender for 5 min to obtain a homogeneous CA solution. The CA solution was cast in 24-well cell culture plates and frozen at −20°C for 8 hrs. The samples were then lyophilized, crosslinked in 0.2 M $CaCl_2$ solution for 10 minutes under vacuum, washed with deionized water several times to remove any excess salt, and sterilized in 70 v% ethanol for 1 hr. The scaffolds were then transferred to a sterile PBS solution and placed on an orbital shaker for > 12 hrs to remove any excess ethanol.

2.3. Cell seeding on scaffolds

Cells were seeded onto PBS damp CA scaffolds in 24-well plates at 50,000 cells per scaffold in 50 μL fully supplemented media. Cells were allowed to infiltrate the scaffold for 1 hr before 1 mL fully supplemented media was added to each well. For Matrigel pre-cultured samples, 50,000 cells in 200 μL fully supplemented media was mixed with 200 μL Matrigel matrix with reduced growth factor and added to 24-well plate wells. Samples were allowed to gel for 1 hr before 1 mL fully supplemented media was added to each well. For 2D pre-cultured samples, 50,000 cells in 1 mL fully supplemented media were added to 24-well plate wells. Media were replaced every 2 days.

2.4 Cell proliferation analysis

Proliferation of cells cultured on 2D wells, matrigel matrix, and CA scaffolds was determined using the Alamar Blue assay following the manufacturer's protocol. Briefly, cells cultured on 2D wells and 3D scaffolds were washed with D-PBS before adding 1 mL of Alamar Blue solution (10% Alamar Blue in fully supplemented phenol red free DMEM) to each well. After 1.5 hrs the Alamar Blue solution was transferred to a 96-well plate to obtain absorbance values on a microplate reader. The cell number was calculated based on standard curves created previously. Cells were again washed with D-PBS to remove Alamar Blue solution and fresh fully supplemented media was added to each well.

2.5 Microscopic analysis

Samples for Scanning Electron Microscopy (SEM) analysis were first fixed with cold Karnovsky's fixative overnight followed by dehydration in a series of ethanol washes (0%, 50%, 75%, 100%, 100%). Samples were critical point dried and sputter coated with platinum before imaging with a JSM 7000 SEM (JEOL, Tokyo, Japan). False color was added to SEM images using Adobe Photoshop in order to improve the contrast between cells and substrate.

2.6 Growth factor and extracellular matrix secretion analysis

After 7 and 9 days of culture for C6 and both U-87 MG and U-118 MG cells, respectively, media of differently cultured cells were replaced with a low serum counterpart (media containing 1% FBS and 1% antibiotic-antimycotic) and cells were incubated for 24 hrs. Media were collected and stored at −80°C for future use. VEGF and MMP-2 secretion was determined following the manufacturer's protocol, protein concentration per cell was calculated based on cell number in the well, and the values were normalized to 2D culture conditions. Laminin and fibronectin were detected using dot blot analyses and protein concentration per cell was normalized to 2D culture conditions using ImageJ.

2.7 In vivo studies

All animal studies were performed in accordance with University of Washington IACUC approved protocols. Athymic nude male mice (nu/nu, 088 strain, Charles River, Wilmington, MA) 6–8 weeks of age were anesthetized with a solution of ketamine and xylazine before CA scaffolds containing cells were implanted subcutaneously into the left and right flank. 2D and Matrigel matrix pre-treated cells were diluted into 100 μL media to a cell number matching that on the CA scaffolds as determined by Alamar blue, and mixed with 100 μL Matrigel before injecting subcutaneously into the left and right flanks of the anesthetized mice. Tumors were measured using calipers and the volume was calculated using the formula of a cylinder, volume = length × width × height × $\pi/4$, for CA scaffold tumors (cell-CA scaffold construct has an cylindrical shape), and using the formula for the volume of an ellipsoid [23], volume =length × (width^2) × $\pi/6$, for 2D and Matrigel tumors. CA scaffold tumor sizes were normalized by subtracting the volume of an empty scaffold (265 mm^3) from the calculated tumor volume. After 3 weeks and 4 weeks of implantation for C6 and U-87 MG tumors, respectively, mice were sacrificed by CO_2 inhalation followed by cervical dislocation, and the tumors were resected, fixed in a 10% formalin solution, and submitted for histological analyses.

2.8 Immunohistochemistry

Excised tumors were embedded in optimal cutting temperature (OCT) compound and frozen on dry ice. The frozen tumor tissue sections (8 μm) were washed thrice with PBS to remove excess OCT compound and fixed for 10 min in formaldehyde. CD31$^+$ cells were stained with an anti-mouse CD31 primary antibody (Abcam, Cambridge, MA) and visualized with an anti-goat IgG FITC conjugated secondary antibody (Abcam, Cambridge, MA) following the manufacturer's protocol. The slides were counterstained with 4',6-diamidino-2-phenylindole (DAPI) in mounting medium (ProLong Gold, Invitrogen, Carsbad, CA) and imaged using a Zeiss LSM 510 confocal microscope.

2.9 Statistical analysis

Acquired data are expressed as mean ± SD. Statistical significance was determined by one-way analysis of variance (ANOVA) and Student's *t* test. Values of $P < 0.01$ were considered significant.

3. Results and Discussion

3.1 Glioma cell incorporation into CA scaffolds

CA scaffolds are prepared by lyophilizing and cross-linking a physical mixture of chitosan and alginate. The formed scaffolds are highly porous to allow for the influx of cells throughout the scaffold, and provide a large surface area for cell attachment and proliferation, ideal for modeling the tumor microenvironment. The tumor model was established by seeding U-87 MG and U-118 MG human glioma cells on the scaffolds and allowing the tumor cells to proliferate *in vitro* for 10 days. A control tumor model was established using C6 rat glioma cells which have a highly malignant phenotype [19–21], and thus should be relatively unresponsive to culture conditions.

Cell incorporation into CA scaffolds was monitored through proliferation and Scanning Electron Microscopy (SEM) analyses. All cell lines were able to proliferate within the CA scaffolds indicating the biocompatibility of the scaffold. Cells were also grown on standard 2D culture wells (24-well plates) and in 3D Matrigel matrix for comparison. The proliferation of cells grown on CA scaffolds was slightly retarded compared to 2D and Matrigel cultures (Fig. 1). This behavior more closely resembles that of tumors *in vivo* which grow more slowly than in standard *in vitro* cell cultures [9]. 2D cultures supply cells with unlimited amounts of

nutrients and sufficient oxygen allowing them to grow rapidly, whereas *in vivo* tumors must recruit blood vessels before they can begin to proliferate rapidly. A slower rate of diffusion of oxygen and nutrients to cells in the interior of the CA scaffolds may account for the retarded growth rate observed, whereas nutrients and oxygen readily diffuse to the interior of the Matrigel gel matrix.

To examine cell morphology, SEM images were acquired of cells grown under the three different conditions (Fig. 2). All three cell lines displayed altered morphologic phenotypes dependent on the culture environment. Cells cultured on 2D wells displayed a linear and elongated morphology, whereas those grown in the 3D culture condition created by the Matrigel matrix developed many invadopodia. Glioma cells cultured on CA scaffolds had a more rounded appearance. Although invadopodia is an indicator of malignancy [24], this morphology is seen in invading cells rather than glioma cells of solid tumors. Cells in solid tumors exhibit a more rounded and interconnected morphology, similar to that seen in cells grown on CA scaffolds. Therefore, the CA scaffolds are able to provide a growth environment that promotes the formation of solid tumor-like cells.

3.2 Differential growth factor expression in cells pre-cultured on CA scaffolds

To determine the effect of 3D culture on the malignant potential of glioma cells, we performed ELISA analyses on the secreted growth factor VEGF (Fig. 3a) and the enzyme MMP-2 (Fig. 3b). Additionally, dot blot analyses were performed to quantify the secretion of extracellular matrix (ECM) proteins, laminin (Fig. 3c) and fibronectin (Fig. 3d). We chose to evaluate these particular growth factors as they play a significant role in angiogenesis and various other pathways in glioma which promote growth, invasion, and resistance to chemotherapeutic drugs [25]. Overexpression of these factors contributes to an increase in cancer malignancy.

VEGF secretion plays a pivotal role in blood vessel recruitment to the tumor [26,27]. As shown in Figure 3a, VEGF secretion by C6 cells grown in CA scaffolds was 0.47 ± 0.16 fold ($P < 0.01$, $N = 3$) lower than those grown on 2D culture wells. U-87 MG cells in CA scaffolds, on the other hand, showed a 13.98 ± 3.58 fold ($P < 0.001$, $N = 3$) higher VEGF secretion than those on 2D culture wells. U-118 MG cells in CA scaffolds also showed an increase in VEGF secretion (1.91 ± 0.50 fold, $P < 0.01$, $N = 3$), as compared to 2D cultured cells.

MMP-2 breaks down the extracellular matrix to provide room for cell proliferation and endothelial cell recruitment for angiogenesis [28]. As shown in Figure 3b, MMP-2 secretion did not change significantly in C6 cells cultured in CA scaffolds, whereas secretion increased 16.24 ± 3.58 fold ($P < 0.0001$, $N = 3$) in U-87 MG cells and 2.17 ± 0.50 fold ($P < 0.01$, $N = 3$) in U-118 MG cells cultured in CA scaffolds as compared to 2D cultures.

Fibronectin and laminin equip cells for angiogenesis by providing a signal and structure for endothelial cell attachment and proliferation [29–31]. Secretion of these extracellular matrix proteins were not significantly changed in C6 cells cultured in CA scaffolds as compared to 2D culture wells, shown in Figures 3c–d. Fibronectin secretion increased 3.13 ± 0.13 fold ($P < 0.0001$, $N = 4$), and laminin secretion increased 1.81 ± 0.01 fold ($P < 0.0001$, $N = 4$) in U-87 MG cells cultured on CA scaffolds as compared to 2D culture wells. For U-118 MG cells cultured on CA scaffolds, fibronectin secretion increased 2.38 ± 0.57 fold ($P < 0.001$, $N = 4$) and laminin secretion increased 5.39 ± 1.19 fold ($P < 0.0001$, $N = 4$) as compared to 2D culture wells. Matrigel samples were not tested since they contain both fibronectin and laminin.

From these data it is apparent that CA scaffolds promote the formation of a more malignant phenotype in human glioma cell lines as compared to standard 2D and Matrigel culture conditions. The up-regulation of growth factors observed upon culture in CA scaffolds indicates these cells have an enhanced ability to modify their extracellular space, and are able

to create a niche conducive to their progression. This behavior is more representative of the human glioma tumor *in vivo* since cells *in vivo* must restructure the extracellular matrix and secrete growth factors to promote angiogenesis. As expected, C6 cells were relatively unresponsive to their environment. This may be due to the fact that this cell line comprises mainly cancer stem cells which favor the expression of factors that promote growth and tumorgenicity, even in standard long-term *in vitro* growth conditions [19,20]. The highly malignant phenotype of C6 cells in standard 2D culture conditions were not further increased upon culture in the 3D environment supplied by either Matrigel matrix or CA scaffolds.

3.3 Tumorigenesis of cells pre-cultured on CA scaffolds

To further assess the malignancy of glioma cells cultured in CA scaffolds as compared to 2D and Matrigel cultures, and to confirm the increase in malignancy was physiologically relevant, the tumorigenicity of U-87 MG cells was determined by implantation of the pre-cultured matrices into nude mice. 2D, Matrigel, and CA scaffold pre-cultured C6 cells were also implanted as a control. As anticipated, C6 cells implanted into mice formed tumors at approximately the same rate regardless of pre-culture condition (Fig. 4a). This is attributable to the minimal difference in growth factor and extracellular matrix secretion in these already highly malignant cells. U-87 MG cells implanted in mice showed a positive correlation between accelerated tumor growth rate and pre-culture in CA scaffolds (Fig. 4b). This increased rate of tumor formation over weeks one ($P < 0.0001$, $N = 6$) and two ($P < 0.0001$, $N = 6$) provides further support that the CA scaffolds were able to mimic the tumor microenvironment as U-87 MG cells were able to develop a malignant profile prior to implantation, allowing for rapid tumor development. However, this rapid tumor growth was not sustained; after an initial burst of tumor growth, the implanted CA scaffold pre-cultured tumors began to grow at a similar rate to the 2D and Matrigel pre-cultured tumors.

Masson's trichrome histological analysis of C6 tumors after 3 weeks of implantation showed no significant changes in cell morphology or deposition of extracellular matrix regardless of pre-culture condition (Fig. 5a), which agrees with the *in vitro* findings. Masson's trichrome histological analysis of U-87 MG tumors 4 weeks following implantation showed an enhanced extracellular matrix secretion in tumors formed from CA scaffold pre-cultured cells (Fig. 5b). This increased deposition of the extracellular matrix provides further evidence of higher malignancy in U-87 MG cells cultured in CA scaffolds.

3.4. Angiogenesis in tumors formed from CA scaffold pre-cultured cells

A key hallmark of malignant tumor progression is angiogenesis. Xenograft tumors formed from 2D cultured cells, Matrigel matrix cultured cells, and CA scaffold cultured cells were photographed in live mice to show vasculature (Fig. 6). Visible blood vessel formation in C6 tumors was not affected by pre-culture conditions as expected from the similarity in growth factor expression levels and tumor growth rate (Fig. 6a). Angiogenesis was highly visible in vasculature to U-87 MG tumors from cells pre-cultured in CA scaffolds (Fig. 6b). No blood vessel recruitment was evident around tumors formed from 2D or Matrigel pre-cultured U-87 MG cells. Even if blood vessels are not visible on the tumor surfaces, endothelial cells can still penetrate the tumor for angiogenesis. To visualize the recruitment of endothelial cells and established blood vessels within the tumors, $CD31^+$ cells were visualized using immunohistochemistry (Fig. 7). There was no apparent difference in $CD31^+$ cell recruitment in C6 tumors regardless of pre-culture condition (Fig. 7a). Further, these cells were randomly distributed throughout the tumor and lacked blood vessel structure. On the other hand, U-87 MG tumors formed from CA scaffold pre-cultured cells showed a greatly enhanced recruitment of $CD31^+$ cells indicating an improved ability for angiogenesis (Fig. 7b). This is further corroborated by the numerous circular blood vessel structures visible in these tumors, whereas the tumors formed from 2D and Matrigel matrix pre-cultured U-87 MG cells showed fewer,

randomly distributed $CD31^+$ cells. This accelerated rate of structured angiogenesis in tumors formed from CA scaffold pre-cultured U-87 MG cells can be attributed to the increased expression levels of growth factors in these cells, indicating their enhanced malignant potential.

We have shown that U-87 MG cells in CA scaffolds exhibited a slower proliferation rate when cultured *in vitro* (Fig. 1), while CA scaffold cultured U-87 MG cells showed accelerated tumor growth *in vivo* (Fig. 4b). This was not unexpected. The proliferation rate *in vitro* is affected by the cells' ability to acquire the oxygen and nutrients which diffuse more slowly in CA scaffolds than on 2D culture plates and Matrigel, which resulted in a slower proliferation rate in CA scaffolds. The tumor growth rate in *vivo* is significantly affected by its ability to recruit blood vessels that provide pathways for biofluid exchange. The results shown in Figure 7b further confirms the correlation between blood vessel formation and tumor growth rate.

4. Conclusions

We have demonstrated that CA scaffolds are able to provide a growth environment for glioma cells *in vitro* which is similar to the tumor microenvironment structure encountered in xenograft tumors *in vivo*. An *in vitro* platform which more accurately represents the tumor microenvironment will undoubtedly expand our understanding of the tumors being studied and play a pivotal role in developing the next generation cancer therapeutics. This reproducible and easily modifiable experimental system offers a number of advantages: they can be easily transferred into mice for rapid xenograft tumor growth, they can be used to pre-screen therapies to reduce the amount of *in vivo* screening, and they can be easily degraded to harvest single, viable cells for analyses such as PCR and flow cytometry. This will not only reduce the amount of time needed to complete experiments, but also reduce the enormous costs and loss of animal life associated with *in vivo* models.

Acknowledgments

This work is supported in part by NIH grants NIH/NCI R01CA119408, R01EB006043, R01CA134213 for MZ and U01CA141539 for MLD. We would like to acknowledge the support of the UW UIF fellowship for FK, and the NIH training grant (T32CA138312) and UW NSF IGERT fellowship for OV. We would also like to acknowledge the use of resources at the Diagnostic Imaging Sciences Center, the Center for Nanotechnology, and the Keck Microscopy Imaging Facility at the University of Washington.

References

1. Mirimanoff RO, Gorlia T, Mason W, Van den Bent MJ, Kortmann RD, Fisher B, et al. Radiotherapy and temozolomide for newly diagnosed glioblastoma: recursive partitioning analysis of the EORTC 26981/22981-NCIC CE3 phase III randomized trial. J Clin Oncol 2006;24:2563–2569. [PubMed: 16735709]
2. Mercer RW, Tyler MA, Ulasov IV, Lesniak MS. Targeted therapies for malignant glioma: progress and potential. BioDrugs 2009;23:25–35. [PubMed: 19344189]
3. Hambley TW, Hait WN. Is anticancer drug development heading in the right direction? Cancer Res 2009;69:1259–1262. [PubMed: 19208831]
4. Smalley KS, Lioni M, Herlyn M. Life isn't flat: taking cancer biology to the next dimension. In Vitro Cell Dev Biol Anim 2006;42:242–247. [PubMed: 17163781]
5. Petersen OW, Ronnov-Jessen L, Howlett AR, Bissell MJ. Interaction with basement membrane serves to rapidly distinguish growth and differentiation pattern of normal and malignant human breast epithelial cells. Proc Natl Acad Sci U S A 1992;89:9064–9068. [PubMed: 1384042]
6. dit Faute MA, Laurent L, Ploton D, Poupon MF, Jardillier JC, Bobichon H. Distinctive alterations of invasiveness, drug resistance and cell-cell organization in 3D-cultures of MCF-7, a human breast cancer cell line, and its multidrug resistant variant. Clin Exp Metastasis 2002;19:161–168. [PubMed: 11964080]

7. Fischbach C, Chen R, Matsumoto T, Schmelzle T, Brugge JS, Polverini PJ, et al. Engineering tumors with 3D scaffolds. Nat Methods 2007;4:855–860. [PubMed: 17767164]
8. Lutolf MP, Hubbell JA. Synthetic biomaterials as instructive extracellular microenvironments for morphogenesis in tissue engineering. Nat Biotechnol 2005;23:47–55. [PubMed: 15637621]
9. Weaver VM, Petersen OW, Wang F, Larabell CA, Briand P, Damsky C, et al. Reversion of the malignant phenotype of human breast cells in three-dimensional culture and in vivo by integrin blocking antibodies. J Cell Biol 1997;137:231–245. [PubMed: 9105051]
10. Kumar S, Weaver VM. Mechanics, malignancy, and metastasis: The force journey of a tumor cell. Cancer Metastasis Rev. 2009
11. Yang Y, Basu S, Tomasko DL, Lee LJ, Yang ST. Fabrication of well-defined PLGA scaffolds using novel microembossing and carbon dioxide bonding. Biomaterials 2005;26:2585–2594. [PubMed: 15585261]
12. Orive G, Tam SK, Pedraz JL, Halle JP. Biocompatibility of alginate-poly-L-lysine microcapsules for cell therapy. Biomaterials 2006;27:3691–3700. [PubMed: 16574222]
13. Hirano S, Seino H, Akiyama Y, Nonka I. Biocompatibility of chitosan by oral and intravenous administration. Crit Rev Ther Drug Carrier Syst 1988;15:143–198.
14. Li Z, Ramay HR, Hauch KD, Xiao D, Zhang M. Chitosan-alginate hybrid scaffolds for bone tissue engineering. Biomaterials 2005;26:3919–3928. [PubMed: 15626439]
15. Li Z, Zhang M. Chitosan-alginate as scaffolding material for cartilage tissue engineering. J Biomed Mater Res A 2005;75:485–493. [PubMed: 16092113]
16. Li Z, Leung M, Hopper R, Ellenbogen R, Zhang M. Feeder-free self-renewal of human embryonic stem cells in 3D porous natural polymer scaffolds. Biomaterials 2010;31:404–412. [PubMed: 19819007]
17. Zheng X, Shen G, Yang X, Liu W. Most C6 cells are cancer stem cells: evidence from clonal and population analyses. Cancer Res 2007;67:3691–3697. [PubMed: 17440081]
18. Shen G, Shen F, Shi Z, Liu W, Hu W, Zheng X, et al. Identification of cancer stem-like cells in the C6 glioma cell line and the limitation of current identification methods. In Vitro Cell Dev Biol Anim 2008;44:280–289. [PubMed: 18594936]
19. Kondo T, Setoguchi T, Taga T. Persistence of a small subpopulation of cancer stem-like cells in the C6 glioma cell line. Proc Natl Acad Sci U S A 2004;101:781–786. [PubMed: 14711994]
20. Cretu A, Fotos JS, Little BW, Galileo DS. Human and rat glioma growth, invasion, and vascularization in a novel chick embryo brain tumor model. Clin Exp Metastasis 2005;22:225–236. [PubMed: 16158250]
21. Chau Y, Padera RF, Dang NM, Langer R. Antitumor efficacy of a novel polymer-peptidedrug conjugate in human tumor xenograft models. Int J Cancer 2006;118:1519–1526. [PubMed: 16187287]
22. Yamaguchi H, Wyckoff J, Condeelis J. Cell migration in tumors. Curr Opin Cell Biol 2005;17:559–564. [PubMed: 16098726]
23. Hoelzinger DB, Demuth T, Berens ME. Autocrine factors that sustain glioma invasion and paracrine biology in the brain microenvironment. J Natl Cancer Inst 2007;99:1583–1593. [PubMed: 17971532]
24. Plate KH, Breier G, Weich HA, Risau W. Vascular endothelial growth factor is a potential tumour angiogenesis factor in human gliomas in vivo. Nature 1992;359:845–848. [PubMed: 1279432]
25. Ferrara N, Carver-Moore K, Chen H, Dowd M, Lu L, O'Shea KS, et al. Heterozygous embryonic lethality induced by targeted inactivation of the VEGF gene. Nature 1996;380:439–442. [PubMed: 8602242]
26. Jouanneau E. Angiogenesis and gliomas: current issues and development of surrogate markers. Neurosurgery 2008;62:31–50. discussion -2. [PubMed: 18300890]
27. Wang F, Weaver VM, Petersen OW, Larabell CA, Dedhar S, Briand P, et al. Reciprocal interactions between beta1-integrin and epidermal growth factor receptor in three-dimensional basement membrane breast cultures: a different perspective in epithelial biology. Proc Natl Acad Sci U S A 1998;95:14821–14826. [PubMed: 9843973]
28. O'Brien LE, Jou TS, Pollack AL, Zhang Q, Hansen SH, Yurchenco P, et al. Rac1 orientates epithelial apical polarity through effects on basolateral laminin assembly. Nat Cell Biol 2001;3:831–838. [PubMed: 11533663]

29. Croft DR, Sahai E, Mavria G, Li S, Tsai J, Lee WM, et al. Conditional ROCK activation in vivo induces tumor cell dissemination and angiogenesis. Cancer Res 2004;64:8994–9001. [PubMed: 15604264]

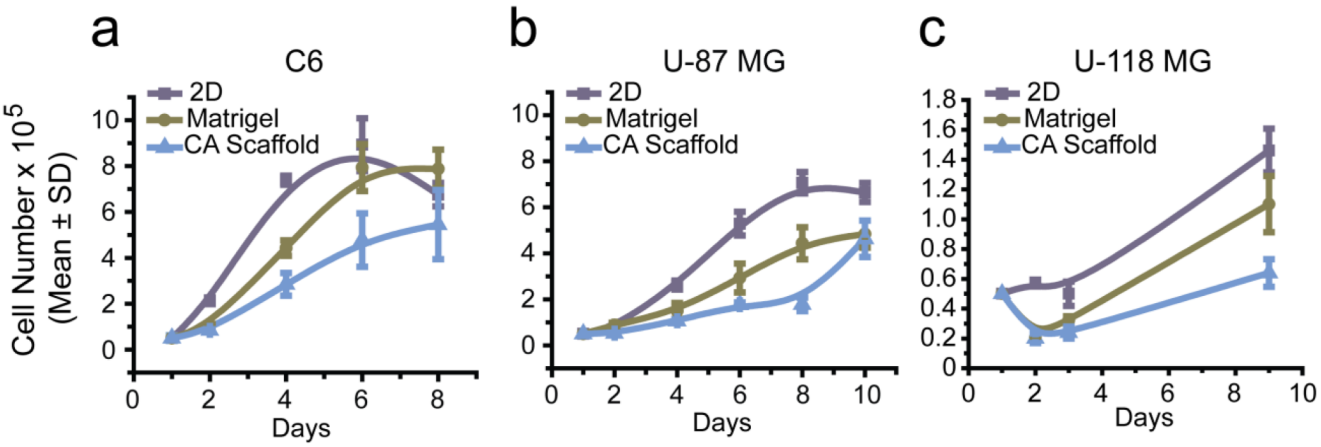

Figure 1.

Ability of CA scaffolds to provide a growth environment for tumor cells *in vitro*. Proliferation of (**a**) C6, (**b**) U-87 MG and (**c**) U-118 MG glioma cells cultured on 2D culture 24-well plates, Matrigel matrix, and CA scaffolds after 2, 4, 6, 8, and 10 days of cell culture, as determined by the Alamar Blue viability assay.

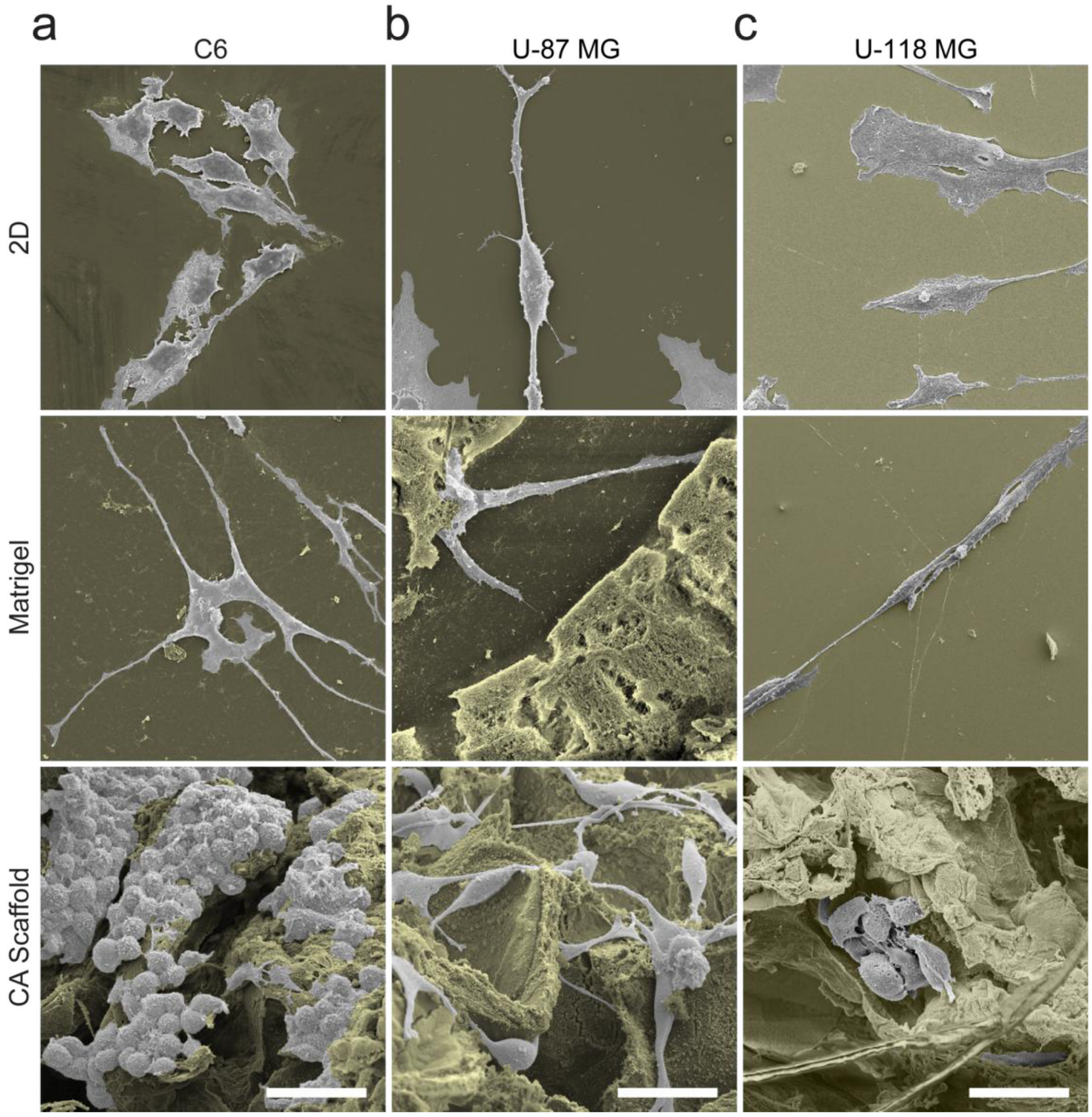

Figure 2.
Morphology of (**a**) C6, (**b**) U-87 MG and (**c**) U-118 MG glioma cells grown on 2D culture plates, Matrigel matrix, and CA scaffolds, visualized by SEM imaging. The background is colored brown for enhanced contrast and the scale bar corresponds to 40 μm.

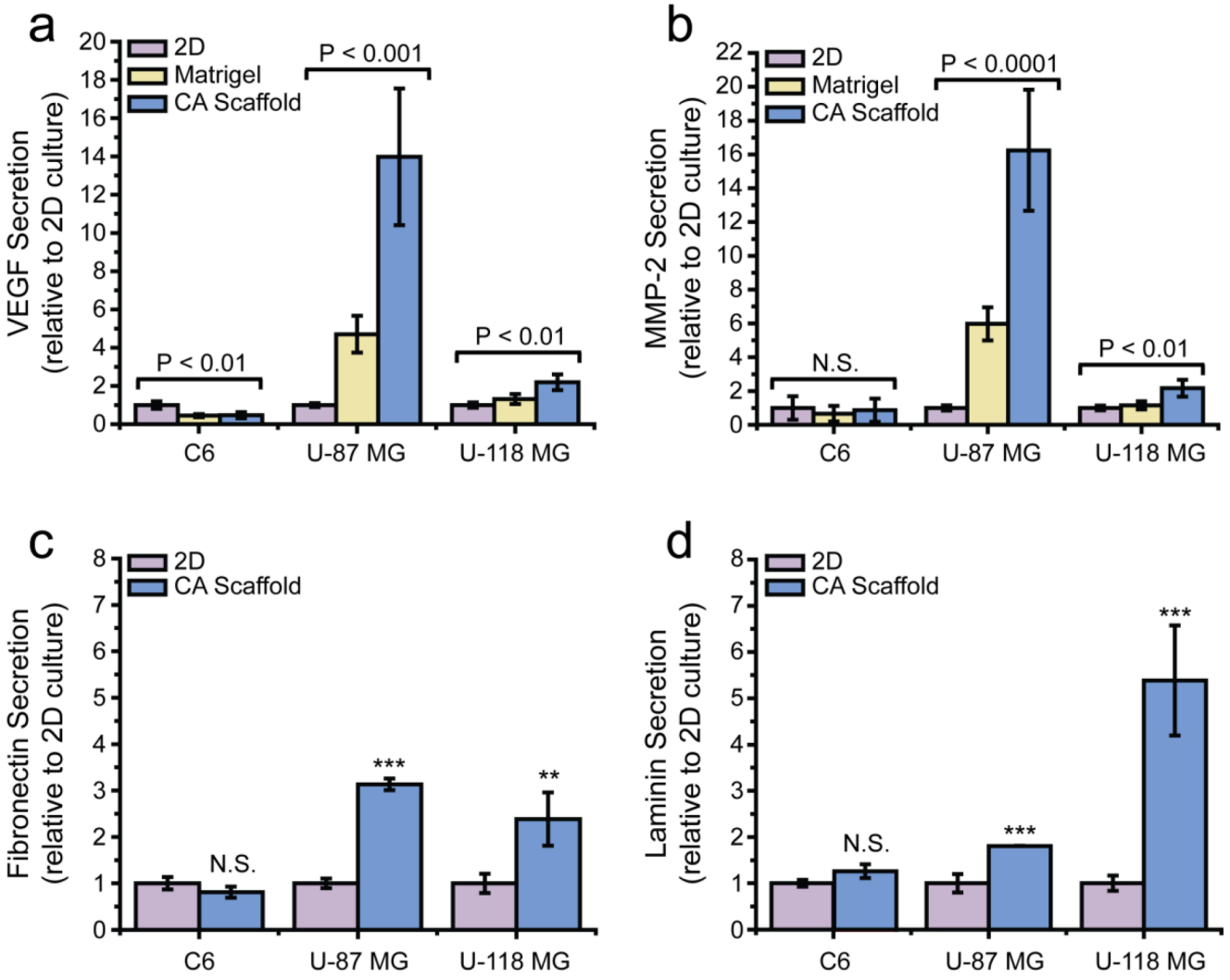

Figure 3.

Phenotypic changes in glioma cells based on *in vitro* pre-culture conditions, assessed by ELISA and dot blot analyses. The secretion of (**a**) VEGF and (**b**) Matrix metalloproteinase-2 in C6, U-87 MG, and U-118 MG cells pre-cultured on 2D 24-well culture plates, Matrigel matrix, and CA scaffolds as determined by ELISA. (**c**) Fibronectin and (**d**) laminin secretion in cells pre-cultured on the three matrices as determined by dot blot analyses. *, $P < 0.01$; **, $P < 0.001$; ***, $P < 0.0001$, by student's t-test ($N = 4$).

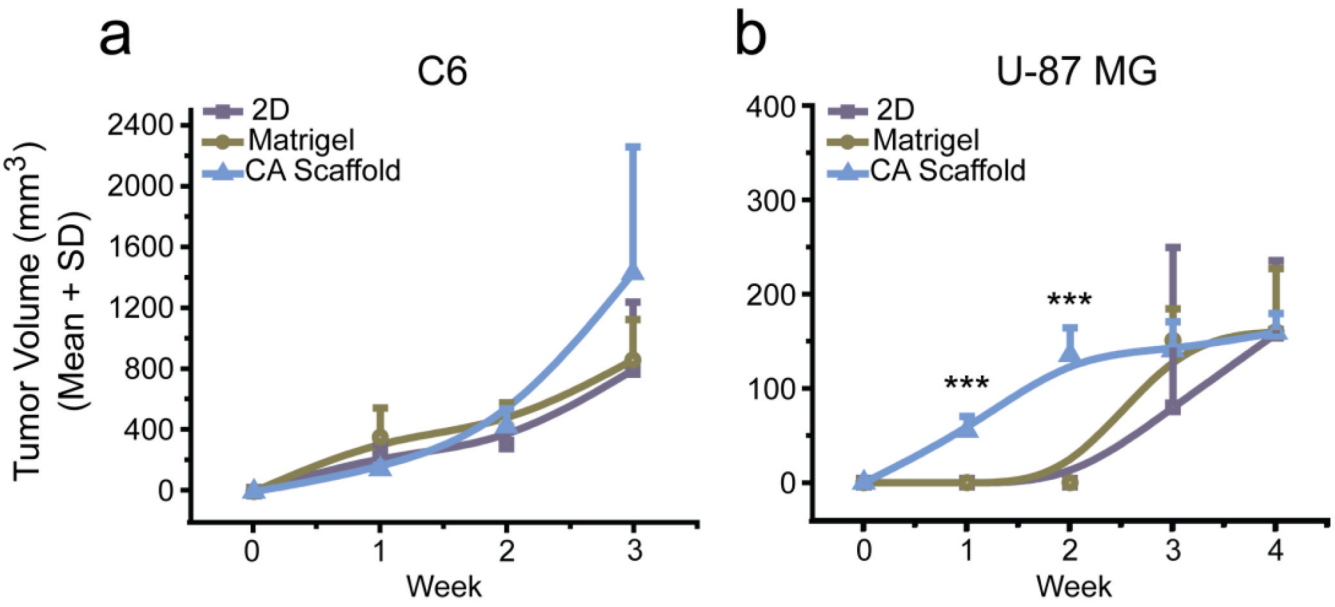

Figure 4.

In vivo study of tumorigenesis of glioma cells pre-cultured under various *in vitro* culture conditions. Growth rates of tumors formed from implants of 2D, Matrigel matrix, and CA scaffold pre-cultured (**a**) C6 or (**b**) U-87 MG cells as determined by caliper measurements. *, $P < 0.01$; **, $P < 0.001$; ***, $P < 0.0001$, by one-way ANOVA ($N = 6$).

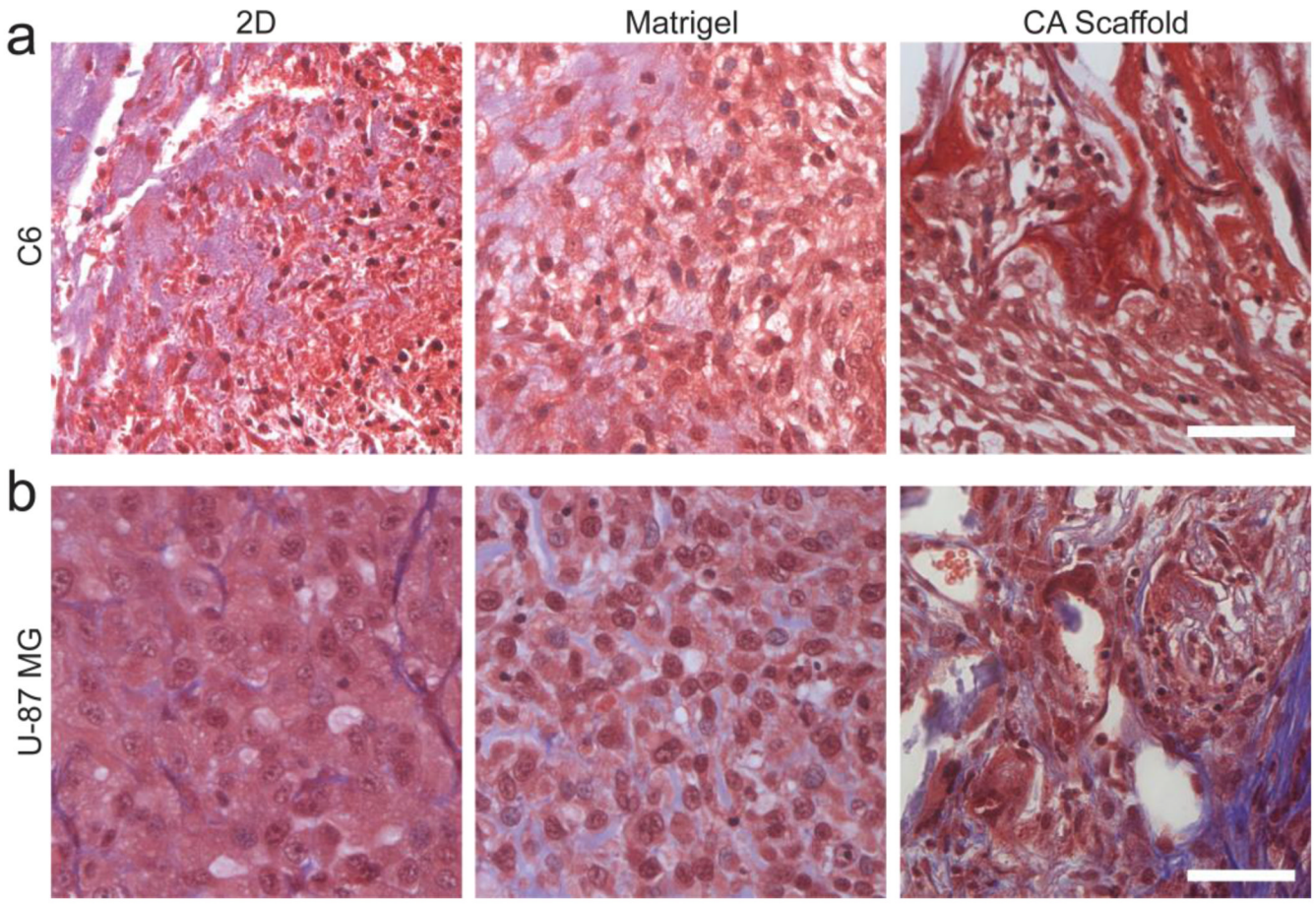

Figure 5.

Histological analysis of glioma tumors grown in athymic nude mice 3 weeks after implantation of pre-cultured glioma cells under various *in vitro* culture conditions.. Masson's trichrome stained histology slides of (**a**) C6 and (**b**) U-87 MG tumors formed from cells pre-cultured on 2D culture 24-well plates, Matrigel matrix, and CA scaffolds. Cell nuclei are stained dark red, cytoplasm is stained light red, connective tissue is stained dark blue, and Matrigel is stained light blue. Scale bar corresponds to 50 μm.

Figure 6.

Angiogenesis around tumors formed from glioma cells pre-cultured on 2D culture 24-well plates, Matrigel matrix, and CA scaffolds. Vasculature surrounding (**a**) C6 and (**b**) U-87 MG tumors were photographed in live, anesthetized mice. Scale bars correspond to approximately 5 mm.

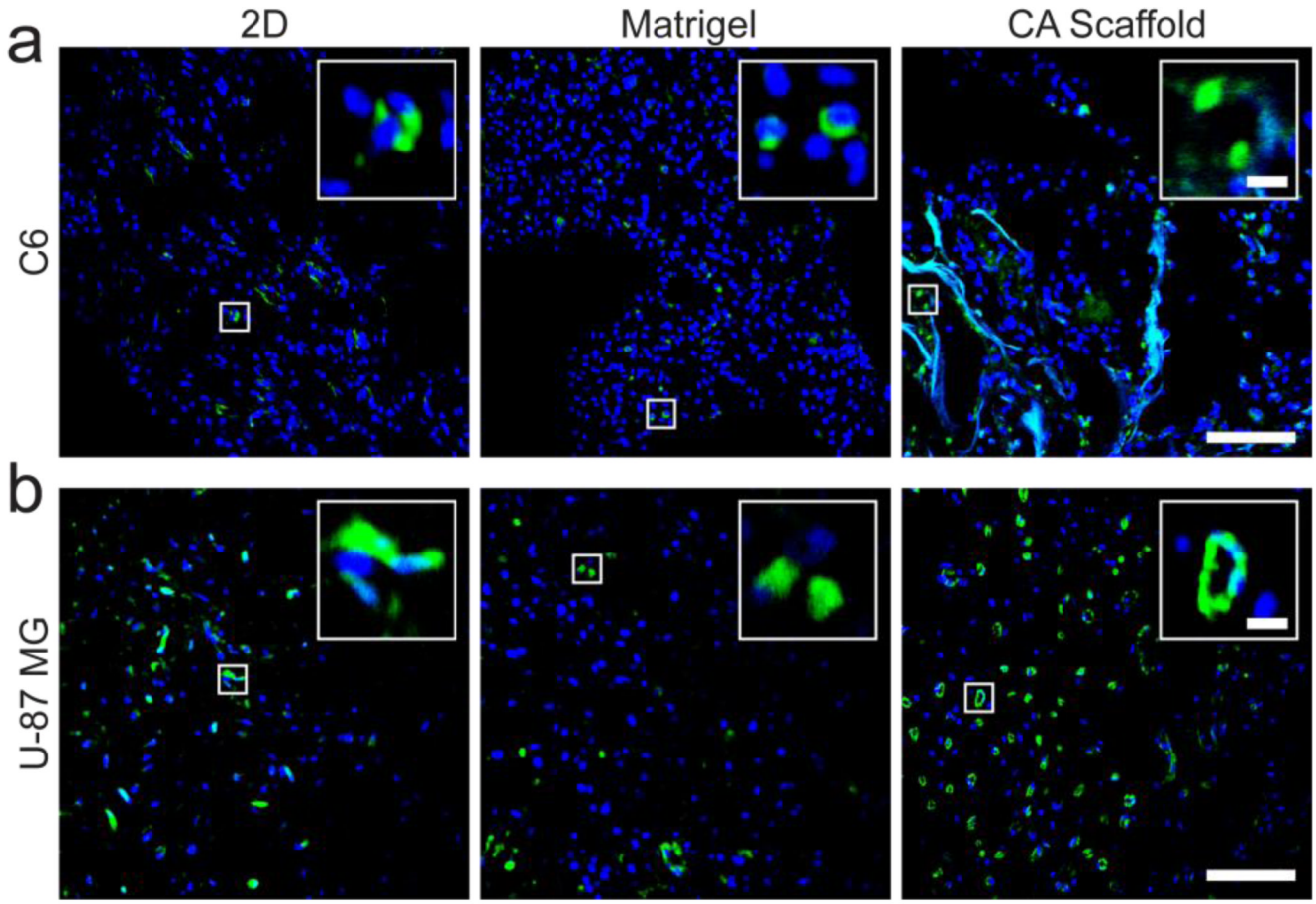

Figure 7.

Immunohistochemistry of tumors grown from glioma cells pre-cultured on 2D culture 24-well plates, Matrigel matrix, and CA scaffolds. (**a**) C6 and (**b**) U-87 MG tumor sections were harvested 3 weeks after implantation of the pre-cultured cells, stained with anti-CD31 to visualize blood vessels (green), and counterstained with DAPI (blue) with inlays to provide more details of the blood vessel structure. Scale bars correspond to 100 μm and 10 μm for the main display and inlay, respectively.